JMEPEG (2012) 21:167–179
DOI: 10.1007/s11665-011-9954-8

1059-9495/$19.00

Shock-Wave Attenuation and Energy-Dissipation Potential of Granular Materials

Mica Grujicic, B. Pandurangan, W.C. Bell, and S. Bagheri

(Submitted February 17, 2011)

The propagation of uniaxial-stress planar shocks in granular materials is analyzed using a conventional shock-physics approach. Within this approach, both compression shocks and decompression waves are treated as (stress, specific volume, particle velocity, mass-based internal energy density, temperature, and mass-based entropy density) propagating discontinuities. In addition, the granular material is considered as being a continuum (i.e., no mesoscale features like grains, voids, and their agglomerates are considered). However, while the granular material is treated as a (smeared-out) continuum, it is recognized that it contains a solid constituent (parent matter), and that the structurodynamic properties (i.e., Equations of State (EOS) and Hugoniot relations) of the granular material are related to its parent matter. Three characteristic shock loading regimes of granular material are considered and, in each case, an analysis is carried out to elucidate shock attenuation and energy dissipation processes. In addition, an attempt is made to identify a metric (a combination of the material parameters) which quantifies the intrinsic ability of a granular material to attenuate a shock and dissipate the energy carried by the shock. Toward that end, the response of a typical granular material to a flat-topped compressive stress pulse is analyzed in each of the three shock loading regimes.

Keywords energy dissipation, granular materials, shock-wave attenuation

1. Introduction

Generation and propagation of shock-waves within granular materials (i.e., natural materials like soils and man-made materials such as metallic and ceramic powders) are an area of intense current research (Ref 1). This interest is driven by a number of factors such as: (a) granular materials are uniquely efficient in attenuating/dispersing shock waves and in dissipating the energy carried by them (Ref 2, 3); (b) novel materials can be produced by shock-induced consolidation of the granular preforms (Ref 4); and (c) unusually high pressures and temperatures are attained in shock-loaded porous materials which provides experimentalists access to the materials in these unique states (Ref 5).

This study deals mainly with the assessment/quantification of the potential of granular materials to attenuate shock and to dissipate the energy carried by such shocks. Materials with a high shock-mitigation capacity (i.e., the ability to efficiently attenuate/disperse shocks and dissipate the energy carried by these shocks) are needed in many military (e.g., mine-blast vehicle survivability, anti-traumatic brain injury head-protection gear), and civilian (e.g., helmets used in sports and recreational activities such as motorcycling, etc.) applications.

Mica Grujicic, B. Pandurangan, W.C. Bell, and **S. Bagheri**, Department of Mechanical Engineering, Clemson University, 241 Engineering Innovation Building, Clemson, SC 29634-0921. Contact e-mail: gmica@clemson.edu.

The extent (and often the temporal evolution) of the shock attenuation process is typically determined using various experimental techniques (Ref 6, 7). However, it is not always clear how the measured data should be handled/processed to estimate/quantify the shock-attenuation/energy-dissipation potential of the material being tested. This problem is particularly compounded in the case of granular materials, whose response may vary greatly with the relative strength (i.e., the ratio of the shock strength as quantified by the peak applied stress/pressure, and the material strength) of the loading shock. In this study, an attempt is made to develop basic guidelines for defining and assessing the shock-attenuation/energy-dissipation capability of granular materials.

The granular material analyzed in this study is treated as a continuum and therefore the mesoscale microstructural aspects (e.g., grain shapes/sizes and their distributions, void shapes/sizes and their distributions, etc.) are not considered. While these details may play a critical role in the process of particle bonding, they are of secondary importance with respect to the phenomena of interest here (e.g., shock wave form, shock speed, etc.). Also as will be made clearer in the subsequent sections, it is often critical to emphasize that a granular material consists of solid material and voids, where the first constituent is referred to as the parent matter.

The response of granular materials to shock loading may be quite complex and involve phenomena such as elastic and inelastic deformation processes, irreversible compaction, phase transformations, and chemical reactions. The analysis presented in this study deals, however, only with inert materials in which no chemical reactions occur as a result of shock loading. In addition, the free energy of the competing structural phases in the material at hand is assumed to be quite high relative to the free energy of the structural phase initially present in the material. Consequently, no provision is given for the

occurrence of phase transformations. Nevertheless, the response of the granular material to shock remains quite complex since it may involve various irreversible energy-dissipative deformation and compaction processes.

As mentioned above, shock propagation in granular materials can involve quite complex phenomena such as irreversible deformation/compaction and phase transformations. However, under certain conditions the analysis of shock propagation in granular materials can be simplified without a significant loss in fidelity of the analysis. Toward that end, it is beneficial to identify three distinct regimes of shock propagation within granular materials:

1.1 Low Granular-Material Strength/Weak-Shock Regime

The (negative) stress ($-t_{11}$) versus specific-volume (v) response of a granular material to uniaxial-strain loading (like the compaction of the material by a piston within a confining cylinder) is depicted schematically in Fig. 1(a). The low-stress, gently sloping part of the loading curve corresponds to the compaction of (i.e., void-elimination within) the granular material. During this process, the granular material specific-volume is reduced from its initial (reference) value, v_R to its fully compacted value, v_{SR}, and subsequently to a fully compacted and compressed value, v_C. Due to the fact that the shock is weak in this loading regime, it is justified to assume that no compression of the parent (solid) material takes place. Thus, one can set $v_C = v_{SR}$. In addition, due to the low strength of the granular material, one can assume that its full compaction is attained at practically zero stress levels. Hence, under these conditions, the stress versus specific-volume (Hugoniot) response of the granular material in this regime can be idealized by a zero stress portion between v_R and v_{SR} and a vertical section at $v = v_{SR}$, Fig. 1(b). In other words, it is postulated that zero stress is required to fully compact the granular material and that no compression of the resulting solid material takes place.

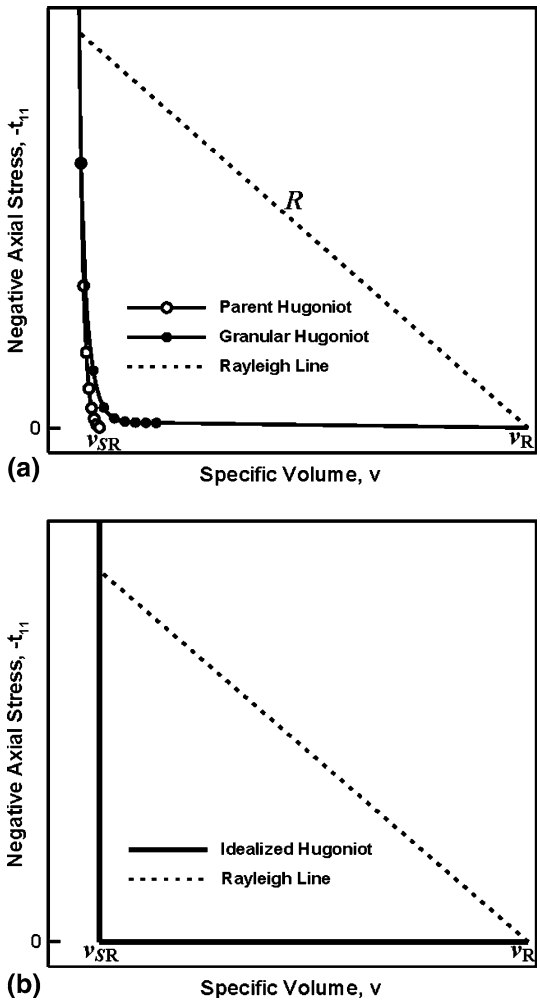

Fig. 1 (a) Typical granular material and its parent matter compression Hugoniots; and (b) an idealization of the granular-material Hugoniot in the low strength/weak-shock regime. In both (a) and (b) an example of the Rayleigh (shock-loading) line is shown

1.2 Strong-Shock Regime

The pressure versus specific-volume responses of the granular material and its parent material in this shock loading regime are depicted in Fig. 2(a). It should be noted that due to the fact that pressures are very high in this shock loading regime and, due to interplay of the compaction processes, the relative magnitude of the stress deviator is small, the pressure is used in place of the $-t_{11}$ (without significant loss of fidelity). The shock is both strong enough to give rise to compression of the fully compacted granular material and sufficiently stronger than the granular-material (so that the details of the granular-material compaction process do not have to be considered). However, this regime of shock loading does not include the highest possible pressures (and temperatures) under which the materials behave in a unique way and the shock physics approach utilized in this study may not be appropriate.

Examination of Fig. 2(a) reveals that the pressure versus specific volume curves of the fully compacted granular and the parent material at the same level of specific volume $v < v_{SR}$ are distinct. The difference between the two curves, as will be explained later, arises from the fact that considerable dissipation of energy (causing an increase in temperature and entropy) is associated with the compaction process within the granular material. Since the shock strength is substantially higher than the granular-material strength, the pressure versus specific-volume curve for the granular material can be idealized by replacing it with a zero-pressure curve in the $v > v_{SR}$ region and assuming that the $v < v_{SR}$ portion of this curve originates from a point corresponding to zero-pressure and $v = v_{SR}$ (the same origination point for the parent matter). The resulting idealized pressure versus specific Hugoniot relation for the porous material along with the corresponding parent matter curve is depicted in Fig. 2(b).

1.3 Moderate-Shock Regime

In this regime, the shock is sufficiently strong to produce both compaction of the granular material and compression of the resulting compacted material. However, since the shock strength is comparable with the granular material strength, details of the compaction process must be considered explicitly. Clearly, the behavior of the material in this regime is substantially more complex than in the other two regimes. Consequently, details of the material response to shock loading in this regime will be presented in the subsequent sections after a number of phenomena and processes associated with irreversible compaction of the granular materials are introduced.

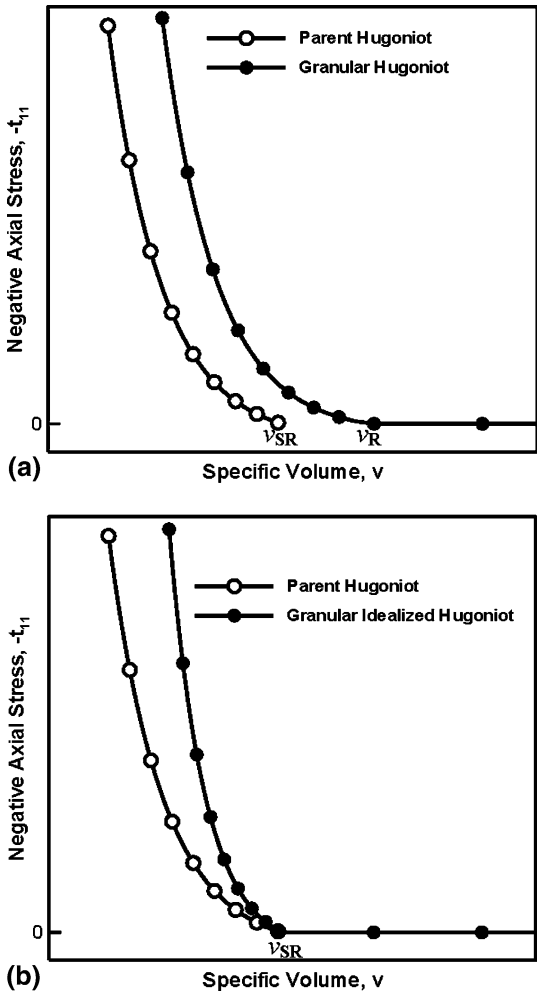

Fig. 2 (a) Typical granular material and its parent matter compression Hugoniots; and (b) an idealization of the granular-material Hugoniot and the parent matter Hugoniot in the strong shock regime

The main objective of this study is to analyze the shock attenuation and energy dissipation phenomena within the granular materials in each of the three shock loading regimes. In each case, an attempt will be made to quantify the shock-attenuation and the energy-dissipation potential of a granular material and relate this potential to the thermo-mechanical properties of the materials. Toward that end, for each of the three regimes mentioned above, the granular material will be assumed to be in the form of a half (semi-infinite) space with $X \geq 0$ subjected to a flat-topped (uniaxial-strain) stress/pressure pulse in the form:

$$t_{11} = \begin{cases} 0, & t < 0 \\ t_{11}^{+} < 0, & 0 \leq t \leq t^{*} \\ 0, & t > t^{*} \end{cases} \qquad \text{(Eq 1)}$$

The amplitude of the stress pulse will be selected in each case, to place the granular material in the shock-loading regime of interest. In each case, the initial state (S^{-}) of the granular material will be defined as: particle velocity, $\dot{x}^{-}$; axial stress $t_{11}^{-} = 0$, $v^{-} = v_{\mathrm{R}}$; mass-based internal-energy density, $\varepsilon^{-} = 0$; temperature, $\theta^{-} = \theta_{\mathrm{R}}$ (=298 K) and mass-based entropy density $\eta^{-} = 0$.

By carrying out the shock-attenuation and energy-dissipation analyses, an attempt will be made to define a metric which can be used in the material selection process where the objective is the selection of granular materials with superb (weight and/or volume-normalized) shock attenuation and energy dissipation potentials.

The organization of the article is as follows. Assessment of the shock attenuation and energy dissipation potentials of the granular materials within the three aforementioned shock loading regimes is presented in section 1, 3, and 4, respectively. The findings obtained are briefly discussed in section 5. The main conclusions resulting from this study are summarized in section 6.

2. Low Granular-Material Strength/Weak-Shock Regime

The analysis presented in this and the next two sections deals with uniaxial-strain longitudinal planar shocks propagating in a semi-infinite medium (i.e., no shock reflection phenomena from the surfaces and the material boundaries are considered).

Both compressive shocks and decompression waves are treated as (stress, energy-density, specific volume, particle velocity, temperature, and entropy-density) propagating discontinuities whose behavior is governed by the three (mass, linear-momentum, and energy) shock jump equations.

2.1 Loading Stage

The initial loading of the granular-material half-space domain by the flat-topped stress/pressure pulse of magnitude t_{11}^{+} described earlier, produces a (compressive) planar shock which compacts the granular material to a specific volume $v^{+} = v_{\mathrm{SR}}$. The remaining quantities defining the material state behind the shock can be obtained using the shock jump equations (Ref 1). The following Eulerian form of the shock jump equations is used in the present work:

$$[\![\rho]\!] u_{\mathrm{s}} = [\![\rho \dot{x}]\!] \qquad \text{(Eq 2)}$$

$$[\![\rho \dot{x}]\!] u_{\mathrm{s}} = [\![\rho \dot{x}^2 - t_{11}]\!] \qquad \text{(Eq 3)}$$

$$\left[\!\left[\rho\left(\varepsilon + \frac{1}{2}\dot{x}^2\right)\right]\!\right] u_{\mathrm{s}} = \left[\!\left[\rho\left(\varepsilon + \frac{1}{2}\dot{x}^2\right)\dot{x} - t_{11}\dot{x}\right]\!\right] \qquad \text{(Eq 4)}$$

where u_{s} represents the Eulerian shock speed, density $\rho = 1/v$, and the $[\![\,]\!]$ denote jumps (i.e., "+" state and "−" state differences) of the designated thermo-mechanical quantities at the shock front. Since t_{11}^{+} is prescribed and $v^{+} = v_{\mathrm{SR}}$, there are only three unknowns ($\dot{x}^{+}$, u_{s}, and ε^{+}) in the three jump equations and these unknowns can be readily obtained by solving Eq 2 to 4 to get:

$$\dot{x}^{+} = \left[(v_{\mathrm{R}} - v_{\mathrm{SR}})(-t_{11}^{+})\right]^{1/2} \qquad \text{(Eq 5)}$$

$$u_{\mathrm{s}} = v_{\mathrm{R}}\left(\frac{-t_{11}^{+}}{v_{\mathrm{R}} - v_{\mathrm{SR}}}\right)^{1/2} \qquad \text{(Eq 6)}$$

$$\varepsilon^{+} = \frac{1}{2}(v_{\mathrm{R}} - v_{\mathrm{SR}})(-t_{11}^{+}) = \frac{1}{2}(\dot{x}^{+})^2 \qquad \text{(Eq 7)}$$

It should be noted that due to the fact that the granular material strength is taken to be zero and that the compacted-material stiffness is assumed to be infinite, shock loading in the present case does not store any strain energy in the material and the internal energy density ε^{+} is of a purely thermal character. In addition, it should be noted that the material behind the shock contains a mass-based kinetic energy density equal to $0.5\dot{x}^{+2}$ which is numerically equal to the mass-based internal energy density, Eq 7. In other words, the work done $\left(-t_{11}^{+}\dot{x}^{+}t^{*}\right)$ by the applied stress at the boundary is equipartitioned between the internal and the kinetic energies of the compacted material.

2.2 Unloading Stage

At the end of the loading pulse, the material is unloaded. In normal materials (i.e., the materials whose stiffness increases continuously with an increase in compressive loading), unloading takes place along an isentrope (emanating from the "+" state) by the propagation of a centered simple wave. However, in the present case, the fully compacted material is assumed to have an infinite stiffness (and thus not compressed) and to be irreversibly compacted. Consequently, unloading takes place at a constant (v_{SR}) level of the specific volume via the propagation of a decompression shock. Since the speed of this shock scales with the slope of the decompression isentrope, it is infinite in the present case. Thus, the decompression shock, once initiated instantaneously catches the leading compression shock and completely attenuates it. This is depicted schematically in Fig. 3(a) in which the Eulerian *x-t* diagram displays the response of a granular material to a flat-topped stress/pressure pulse. Figure 3(b) and (c) shows the stress-based shock wave fronts at two different times preceding the initiation of the release shock. During this process, the material particles are brought to rest, i.e., the kinetic energy present in the "+" state of the material is dissipated in the form of heat. In other words, the entire work done by the stress pulse on the boundary is converted to heat. This causes a temperature rise of $\dot{x}^{+2}/C_{SR}^{v}$, where C_{SR}^{v} is the constant volume specific heat of the parent material. Clearly, to minimize the risk of over-heating, materials with a larger value of C_{SR}^{v} (as well as with a larger maximum service temperature) are preferred.

2.3 Weak Shock-Attenuation/Energy-Dissipation Potential of Granular Materials

To summarize, the granular materials in this regime behave as a perfect shock-wave attenuators and energy dissipaters provided the thickness of the material is large enough to enable shock annihilation before the leading compression shock reaches the back-face of the granular material. Such critical thickness $(= u_s t^{*})$, for a given duration *t** of the loading pulse can be reduced in the case of the granular materials by lowering the shock speed, u_s. As defined by Eq 6, the shock speed scales with the square-root of the slope of the Rayleigh line, labeled as "*R*" in Fig. 1(a). This slope can be reduced, for a given choice of the shock strength $\left(t_{11}^{+}\right)$ and the parent matter (v_{SR}) by increasing the initial specific volume, v_R, of the granular material. However, there is a limit for the v_R increase and beyond such limit the granular material starts behaving as an aggregate of loosely interacting discrete particles and the current continuum-based approach breaks down. In any case, materials with a large value of v_R-v_{SR} are preferred from the standpoint of shock-attenuation and energy-dissipation. If one assumes that if the maximum value of v_R at which the current theory breaks down can be defined as $c * v_{SR}$, where c is a material independent coefficient, then materials with a large value of v_{SR} are preferred. Since this implies that low density ($\rho_{SR} = 1/v_{SR}$) materials are preferred, the selection of large v_{SR} materials is beneficial to the fulfillment of the often accompanying low weight requirement.

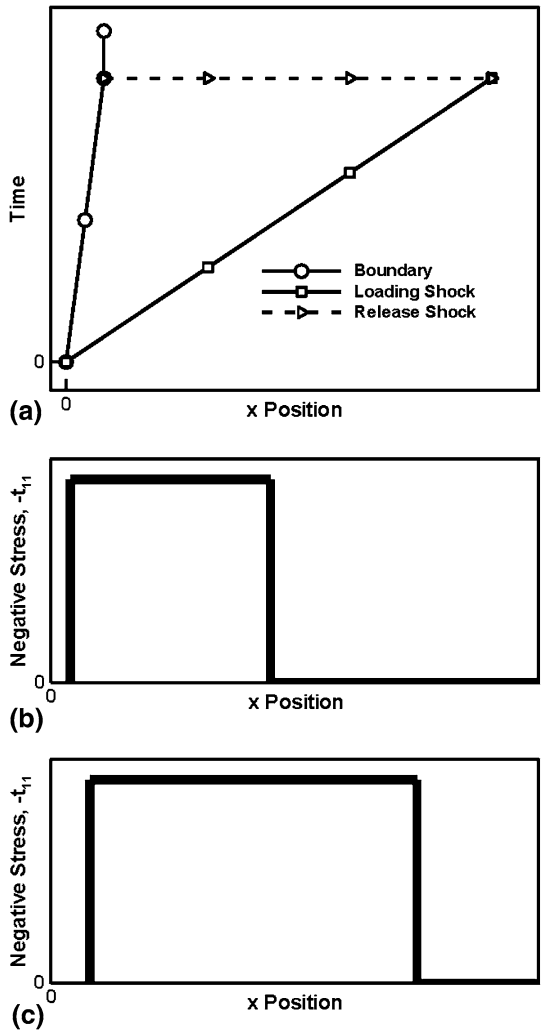

Fig. 3 (a) Eulerian trajectories of the granular-material boundary, compression shock, and the release shock in the low-strength weak-shock regime; (b, c) the resulting stress-based shock profiles at two different times before initiation of the release shock

As mentioned above, in this shock-loading regime, granular materials behave as ideal shock-attenuators and energy-dissipaters. However, in practice this regime (commonly referred to as the "snow-plowing" regime) is not readily attained since typically material strength increases during the compaction process and may become comparable to the shock strength (invalidating the low-strength assumption governing this shock-loading regime).

3. Strong-Shock Regime

As mentioned earlier, shock strength is so much higher than the material strength in this regime that details of the

compaction process can be neglected and the granular material may be considered to be in a fully compacted state (from the onset of the analysis). However, it should be noted that the pressures in this regime are not extreme and, hence, the basic thermodynamic relations (e.g., the Mie-Gruneisen equation of state, Rankine-Hugoniot equation, etc.) can be employed. In other words, this regime does not include the highest possible pressures and temperatures at which materials may display some unique properties (see (Ref 8)) and at which the use of the aforementioned thermodynamic relations may not be justified.

Also it should be noted that due to high shock strength, the contribution of the stress deviator to t_{11} is relatively small and, hence, the axial stress, t_{11}, can be replaced by negative pressure, $-p$, without significant loss in fidelity of the analysis.

3.1 Loading Stage

When analyzing the behavior of granular materials in this shock loading regime, one generally encounters first the problem of determination of the stress/pressure versus specific volume (as well as other Hugoniot) relations for the fully compacted granular material from the known corresponding Hugoniot relations for the parent material. The typical procedure used in this situation is described below.

The procedure involves the following steps:

(a) A standard p-v-ε Mie-Gruneisen Equation of State (EOS) is first used to relate the granular material Hugoniot pressure, $p^{(\mathrm{H})}(v)$, and mass-based energy density, $\varepsilon^{(\mathrm{H})}(v)$, to their parent material counterparts, $p^{(\mathrm{HS})}(v)$ and $\varepsilon^{(\mathrm{HS})}(v)$ as:

$$p^{(\mathrm{H})}(v) = p^{(\mathrm{HS})}(v) + \frac{\gamma(v)}{v}\left[\varepsilon^{(\mathrm{H})}(v) - \varepsilon^{(\mathrm{HS})}(v)\right] \qquad \text{(Eq 8)}$$

where $\gamma(\mathrm{v})$ is the so called Gruneisen Gamma (a material parameter which relates an increase in pressure with an increase in the internal energy density) and is given by

$$\gamma(v) = \gamma_{\mathrm{SR}}\frac{v}{v_{\mathrm{SR}}} \qquad \text{(Eq 9)}$$

where γ_{SR} is the Gruneisen gamma for the parent matter in the reference state.

It should be noted that in Eq 8, it is postulated that the thermo-mechanical behavior of the parent material and that of the fully compacted granular material are defined by the same p-v-ε Mie-Gruneisen EOS. Simply stated, the p-v-ε Mie Gruneisen EOS represents a surface in the p-v-ε space, while the two Hugoniots denote two closely spaced lines lying on this surface. There are three unknown functions, $p^{(\mathrm{HS})}(v)$, $\varepsilon^{(\mathrm{H})}(v)$, and $\varepsilon^{(\mathrm{HS})}(v)$ on the right-hand side of Eq 8. These functions must be defined before $p^{(\mathrm{H})}(v)$ can be evaluated.

(b) First, the function $p^{(\mathrm{HS})}(v)$ is defined by combining the known Eulerian shock speed relation $u_s = C_{\mathrm{B}} + S\dot{x}^{+} + \dot{x}^{-}$ (C_{B} and S are known parent material constants) with the three shock jump conditions, Eq 2 to 4 (e.g. (Ref 1)) to obtain:

$$p^{\mathrm{HS}}(v) = \frac{(\rho_{\mathrm{R}}C_{\mathrm{B}})^2(v_{\mathrm{R}} - v)}{[1 - \rho_{\mathrm{R}}S(v_{\mathrm{R}} - v)]^2}. \qquad \text{(Eq 10)}$$

(c) The two energy density functions appearing in Eq 8 are related to their respective pressure functions by the corresponding Rankine-Hugoniot equations (Ref 1) as:

$$\varepsilon^{(\mathrm{H})}(v) = \varepsilon_{\mathrm{R}} + \frac{1}{2}p^{(\mathrm{H})}(v)(v_{\mathrm{R}} - v) \qquad \text{(Eq 11)}$$

$$\varepsilon^{(\mathrm{HS})}(v) = \varepsilon_{\mathrm{SR}} + \frac{1}{2}p^{(\mathrm{HS})}(v)(v_{\mathrm{SR}} - v) \qquad \text{(Eq 12)}$$

where the quantities labeled with subscript "R" and "SR" are the known minus-state material quantities for the granular material and its parent matter, respectively.

(d) Equation 10 to 12 is then combined to get the sought $p^{(\mathrm{H})}(v)$ Hugoniot for the granular material in terms of the known $p^{(\mathrm{HS})}(v)$ Hugoniot of the parent material as:

$$p^{(\mathrm{H})}(v) = \frac{1 - \frac{\gamma(v)}{2v}(v_{\mathrm{SR}} - v)}{1 - \frac{\gamma(v)}{2v}(v_{\mathrm{R}} - v)}p^{(\mathrm{HS})}(v) \qquad \text{(Eq 13)}$$

where $p^{(\mathrm{HS})}(v)$ is defined by Eq 10.

An example of the results obtained in this portion of the study is presented in Fig. 4(a) in which pressure versus specific volume Hugoniot relations are depicted for granular copper $v_{\mathrm{R}} = 1.5v_{\mathrm{SR}}$ and for the solid copper (C_{B} = 3940 m/s, S = 1.489, γ_{SR} = 1.99, v_{SR} = 1/8930 m^3/kg).

(e) The energy density Hugoniot for the fully compacted granular material is then obtained by substituting Eq 13 into 11.

(f) Finally, the associated Eulerian shock speed can be obtained by combining the first two shock jump equations with the previously determined $p^{(\mathrm{H})}(v)$ relation to get:

$$u_s = v_{\mathrm{R}}\left(\frac{p^{(\mathrm{H})}(v)}{v_{\mathrm{R}} - v}\right)^{1/2} + \dot{x}^{-} \qquad \text{(Eq 14)}$$

At this point, the pressure Hugoniot for the granular material is determined. However, to address the potential of overheating, the corresponding temperature Hugoniot is also required for this material. In addition, since unloading takes place along an isentrope, the entropy density Hugoniot is also required.

To determine the temperature Hugoniot for the granular material (as well as for the parent matter) from the known corresponding pressure Hugoniot, the procedure described in Appendix is used. This procedure yielded:

$$\theta^{(\mathrm{H})}(v) = \chi(v)\left[\frac{\theta_{\mathrm{R}}}{\chi(v_{\mathrm{SR}})} + \frac{1}{2C_{\mathrm{R}}^{v}}\int_{v_{\mathrm{SR}}}^{v}\frac{k(v')}{\chi(v')}\mathrm{d}v'\right] \qquad \text{(Eq 15)}$$

where the function $k(\upsilon)$ will be defined in the Appendix while the function $\chi(\upsilon)$ is defined in Eq 22.

An example of the results obtained in this portion of the study is presented in Fig. 4(b) in which temperature versus specific volume Hugoniot relations are depicted for granular copper $v_{\mathrm{R}} = 1.5v_{\mathrm{SR}}$ and for the solid copper.

To determine the entropy Hugoniot for the granular material (as well as for the parent matter) from the known corresponding pressure Hugoniot, Eq A.4 is integrated to yield:

$$\eta^{(\mathrm{H})}(v) = \eta_{\mathrm{R}} + \frac{1}{2}\int_{v_{\mathrm{SR}}}^{v}\frac{k(v')}{\theta^{(\mathrm{H})}(v')}\mathrm{d}v' \qquad \text{(Eq 16)}$$

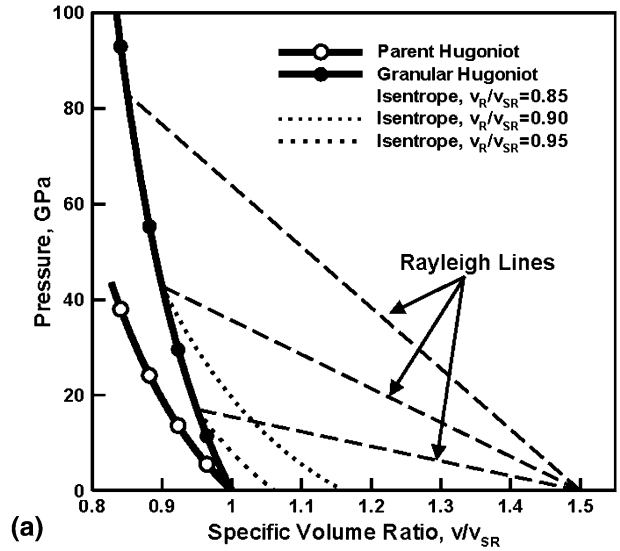

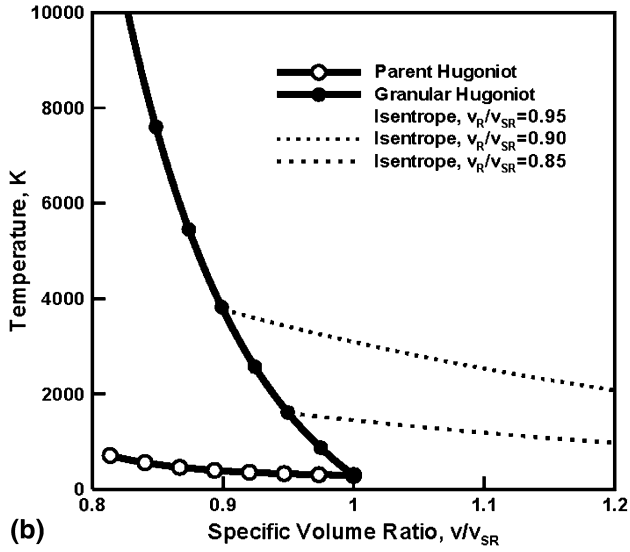

Fig. 4 (a) The pressure and (b) the temperature Hugoniots and decompression isentropes for granular copper with an initial degree of distention of v_R/v_{SR} = 1.5

3.2 Unloading Stage

As stated earlier, in a normal material, impulsive compressive-loading takes place along the corresponding Rayleigh line and the locus of the (shock-strength dependent) "+" states is defined by the corresponding Hugoniot relation. In this case, impulsive compressive-loading is introduced into the material by a (leading) compression shock. In the same kind of materials, the effect of decompression is introduced into the material by the propagation of a spread-out centered simple wave and unloading takes place along an isentrope.

To determine the unloading pressure isentrope, $p^{(\eta)}(v)$, and the corresponding energy-density isentrope, $\varepsilon^{(\eta)}(v)$, the following procedure is utilized:

(a) The (unknown) isentropes and the (known) Hugoniots for the compacted granular material are mutually related by the p-v-ε Mie-Gruneisen equation of state in the form:

$$p^{(\eta)}(v) = p^{(H)}(v) + \frac{\gamma_{SR}}{v_{SR}}\left[\varepsilon^{(\eta)}(v) - \varepsilon^{(H)}(v)\right]. \qquad \text{(Eq 17)}$$

(b) Next, the (unknown) energy and pressure isentropes for a compacted material, Eq 17 are mutually related via the energy balance equation given by:

$$\varepsilon^{(\eta)}(v) = \varepsilon^{+} - \int_{v^{+}}^{v} p^{(\eta)}(v', \eta^{+})\, dv' \qquad \text{(Eq 18)}$$

where "+" is used to denote the (known) quantities in the shock-loaded "+" state of the fully compacted and compressed granular material.

(c) After substitution of Eq 18 into 17 and differentiation of the resulting equation with respect to v, the following first-order ordinary differential equation is obtained:

$$\frac{dp^{(\eta)}(v)}{dv} + \frac{\gamma_{SR}}{v_{SR}} p^{(\eta)}(v) = k(v) \qquad \text{(Eq 19)}$$

where $k(v)$ is given by:

$$k(v) = \frac{\gamma_{SR}}{2v_{SR}} p^{(H)}(v) + \left[1 - \frac{\gamma_{SR}}{2}\left(\frac{v_R}{v_{SR}} - \frac{v}{v_{SR}}\right)\right]\frac{dp^{(H)}(v)}{dv} \qquad \text{(Eq 20)}$$

Please note that $k(v)$ used in this section, Eq 20 has a different definition than its loading counterpart appearing in Eq A.4.

(d) The solution to Eq 19 that satisfies the initial condition $p^{(\eta)}(v^{+}, \eta^{+}) = p^{+}$ is given by:

$$p^{(\eta)}(v, \eta^{+}) = \chi(v)\left[\frac{p^{+}}{\chi(v^{+})} + \int_{v^{+}}^{v} \frac{k(v')}{\chi(v')} dv'\right] \qquad \text{(Eq 21)}$$

where $\chi(v)$ is

$$\chi(v) = \exp\left[\frac{\gamma_{SR}}{v_{SR}}(v_R - v)\right] \qquad \text{(Eq 22)}$$

An example of the results obtained in this portion of the study is presented in Fig. 4(a) in which pressure versus specific volume isentropes are depicted for granular copper $v_R = 1.5v_{SR}$ compacted to specific volumes of $v_R(=v/v_{SR}$ = 0.95, 0.9, and 0.85).

(e) The corresponding energy isentrope is then defined by Eq 18.

(f) As mentioned earlier, the effect of decompression is propagated into the material by a spread-out simple wave. The leading and the trailing portions of this wave advance into the material at a velocity:

$$c_L^{(\eta)}(v) = \left(\frac{dp^{(\eta)}(v)}{dv}\right)^{\frac{1}{2}} + \dot{x}^{-} \qquad \text{(Eq 23)}$$

where the $\left(\frac{dp^{(\eta)}(v)}{dv}\right)$ term is evaluated at $p^{(\eta)} = p^{+}$ and $p^{(\eta)} = 0$, respectively.

The last point to be addressed in this portion of the analysis deals with the determination of the temperature isentrope.

Toward that end, advantage is taken of the alternative definition of the Gruneisen gamma, $\gamma = -v\left.\frac{\partial\left[\ln\left(\frac{\theta}{\theta_R}\right)\right]}{\partial v}\right|_{\eta}$ to get:

$$\theta^{(\eta)}\left(v', \eta^{+}\right) = \theta^{+}\exp\left[\gamma_{SR}\left(\frac{v^{+}}{v_{SR}} - \frac{v}{v_{SR}}\right)\right] \quad \text{(Eq 24)}$$

An example of the results obtained in this portion of the study is presented in Fig. 4(b) in which temperature versus specific volume isentropes are depicted for granular copper $v_R = 1.5v_{SR}$ compacted to specific volumes of $v_R(=v/v_{SR} =$ 0.95, 0.9, and 0.85).

3.3 Strong Shock-Attenuation/Energy-Dissipation Potential of Granular Materials

Examination of the results depicted in Fig. 4(a) shows that the speed of the leading portion of the decompression wave is higher while that of the trailing portion of the decompression wave is lower than the compression shock speed only under the strongest shock conditions analyzed. As will be shown below, with the exception of the strongest shock case, the entire centered simple wave will be able to overtake the shock and annihilate it.

The compression shock will be first captured by the leading portion of the decompression wave and this will take place at a time defined by the condition: $u_s(v^{+}) \cdot t = c_L^{\eta}(v^{+})(t - t^{*})$. Past this point, subsequent portions of the decompression wave will also arrive at the shock front causing its strength to decrease (shock attenuation effect). As the shock strength decreases, shock speed also decreases allowing additional portions of the decompression wave to overtake the shock. In the cases other than the strongest shock case analyzed, the entire decompression wave will be able to overtake the shock and annihilate it. In sharp contrast, in the strongest shock case analyzed, the trailing portion of the decompression wave will always move at a velocity which is lower than shock speed. In this case, complete shock attenuation takes place after an infinite amount of time when the distance between the shock-front and the trailing portion of the decompression wave is infinite. An example of the shock attenuation results associated with the strongest shock regime analyzed are displayed in Fig. 5. Careful examination of this figure shows that the shock speed decreases as the shock is attenuated, the trailing portion of the decompression wave moves with a constant velocity and the separation distance between the shock front and the training portion of the wave decreases.

A convenient measure of the shock attenuation potential of a granular material is the minimal distance travelled by the compression shock before it is fully annihilated. In the strongest shock case analyzed, this distance has to be replaced with the one corresponding to the distance travelled by the shock at which the shock strength falls below an acceptable threshold level. This distance is affected by both the shock speed and the (average) speed of the centered simple wave. A material with superb shock attenuation potential should possess a combination of the low shock speed and a high decompression wave speed. A low shock speed can be achieved, in accordance with the analysis presented in the weak-shock section, by choosing highly distended materials with a large value of v_{SR}. In addition, granular materials based on parent matter with low values of C_B and S are preferred from the standpoint of attaining low shock speeds. As far as attaining the high decompression wave speed is concerned, a parametric analysis carried out in this study revealed that materials with low values of γ_{SR}/v_{SR} are preferred.

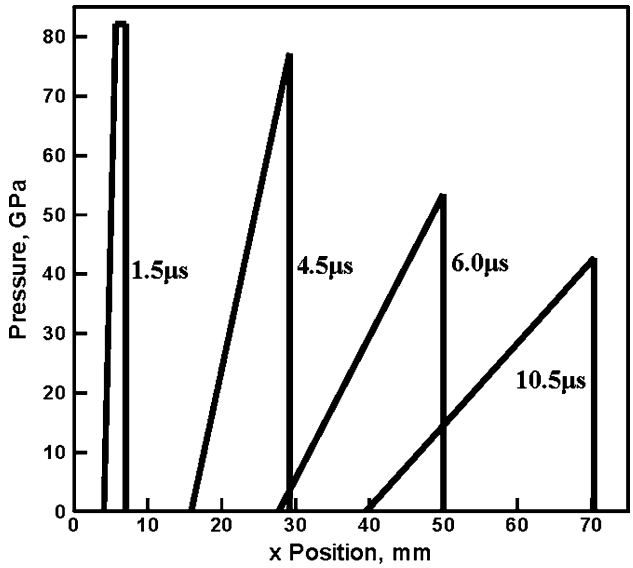

Fig. 5 A sequence of pressure-distance waveforms illustrating shock attenuation in the strong-shock regime for granular copper with an initial degree of distention of $v_R/v_{SR} = 1.5$. The time corresponding to each waveform is given by the association number on the figure

As far as the energy dissipation potential of the granular material is concerned, it relates graphically to the area in the pressure versus specific volume diagram, Fig. 4(a), defined by the loading Rayleigh line, unloading isentrope and the zero pressure axis. The dissipated energy-density in question can be obtained by subtracting from the Hugoniot internal energy density corresponding to the "+" state, Eq 11, the isentrope internal energy density associated with zero pressure, Eq 18. Careful examination of the energy-dissipation potential revealed that the combinations of material properties which promote shock attenuation are also conducive to the energy dissipation process.

Finally, to address the issues associated with the granular-material overheating, materials with large values of the specific heat and the maximum service temperature are preferred.

4. Moderate-Shock Regime

In this regime of shock loading, both the compaction of the granular material and the compression of the resulting (partially) compacted granular material have to be considered. In addition, details of the compaction process and the behavior of the partially compacted granular material have to be taken into account. Specifically, ductile granular materials are considered here which at low stresses respond elastically while at sufficiently high stresses tend to undergo pressure and shear-induced inelastic deformations leading to compaction. Under the assumption that inter-granular friction is quite low, the effect of macroscopic shear stresses can be neglected and the compaction process (involving rearrangement and plastic deformation of granules of parent material) will be assumed to be controlled by pressure alone.

4.1 Loading Stage

As in the case of the strong shock regime, the main task in this portion of the analysis is to derive the Hugoniot relations for the (partially compacted) granular material. However, as explained above, this procedure is substantially more complex in the present case due to the presence of a partially compacted material (which undergoes further compaction and compression during additional loading). The first step toward deriving the sought Hugoniot relations is to derive the associated Equation of State.

4.1.1 Derivation of the Granular Material Equation of State. As mentioned above, the first task encountered in this portion of the study is the derivation of the equation of state for the granular material from the known equation of state for the parent material. Toward that end, the so-called p-α theory originally proposed by Hermann (Ref 9) will be adopted. Within this theory, the volume of a unit mass of the granular material is considered to be the sum of the volume of the solid/parent material and the volume of the voids. No mesoscale microstructural features of the granular material such as the size or shape of individual voids, the distribution of void sizes, etc., are considered and, due to extremely small tensile strength of the granular material, the theory is limited to the compressed states of the material.

Within the p-α theory, the state of a partially compacted granular material is described in terms of the following three state variables v, η and α, where porosity α is defined as:

$$\alpha = \frac{v}{v_s} \tag{Eq 25}$$

where v_s is the specific volume of the solid/parent material at the prevailing thermodynamic state of the granular material.

The basic premise of the p-α theory is that at the same level of $v_s(=v/\alpha)$ the (partially) compacted granular material and its parent material have identical internal energy densities, i.e.,

$$\varepsilon_s\left(v_s = \frac{v}{\alpha}, \eta\right) = \varepsilon(v, \eta, \alpha) \tag{Eq 26}$$

It should be noted that Eq 26 assumes that the contribution of surface energy to the solid-material internal energy within the granular material is small and that it can be neglected.

Since the internal energy density serves as a thermodynamic potential for pressure and temperature,

$$p = -\frac{\partial \varepsilon(v, \eta)}{\partial v} \tag{Eq 27}$$

$$\theta = \frac{\partial \varepsilon(v, \eta)}{\partial \eta} \tag{Eq 28}$$

the pressure and the temperature equations of state for the granular material can be defined as:

$$p(v, \eta, \alpha) = -\frac{\partial \varepsilon(v, \eta, \alpha)}{\partial v} = -\left.\frac{\partial \varepsilon_s}{\partial v_s}\right|_\eta \frac{\partial v_s}{\partial v} = -\frac{1}{\alpha}\left.\frac{\partial \varepsilon_s}{\partial v_s}\right|_\eta = \frac{1}{\alpha} p_s(v_s = v/\alpha, \eta) \tag{Eq 29}$$

$$\theta(v, \eta, \alpha) = \frac{\partial \varepsilon(v, \eta, \alpha)}{\partial \eta} = \frac{\partial \varepsilon_s(v/\alpha, \eta)}{\partial \eta} = \theta s(v_s = v/\alpha, \eta) \tag{Eq 30}$$

Next, it is assumed that the equation of state (the complete Mie Gruneisen EOS, in the present case) for the parent material is known and that the reference state of this material is defined as: $p = 0$, $\varepsilon = \varepsilon_R$, $\eta = \eta_R$, $\theta = \theta_R$, and $v_S = v_{SR}$.

The known complete Mie-Gruneisen energy equation of state for the parent material is given as (Ref 1):

$$\varepsilon_s(v_s, \eta) = \varepsilon_R + \varepsilon_s^{(\eta)}(v_s; \eta_R) + C_{SR}^v \theta_R \chi_c(v_s)[\omega_c(\eta) - 1] \tag{Eq 31}$$

where $\varepsilon_s^{(\eta)}(v_s; \eta_R)$ is the energy isentrope associated with η_R, C_{SR}^v is the specific heat at constant volume for the parent material and the functions $\chi_c(v_s)$ and $\omega_c(\eta)$ are defined as:

$$\chi_c(v_s) = \exp\left[\frac{\gamma_{SR}}{v_{SR}}(v_{SR} - v_s)\right] \tag{Eq 32}$$

$$\omega_c(\eta) = \exp\left[\frac{\eta - \eta_R}{C_{SR}^v}\right] \tag{Eq 33}$$

It should be noted that in Eq 31, 32, and 33 the following assumptions were made: $C_s^v = C_{SR}^v$ and $\gamma(v_s) = \frac{\gamma_{SR}}{v_{SR}} v_s$. These assumptions are reasonable considering the fact that at typical pressures of a few gigapascals encountered in this shock-loading regime, the associated thermal effects are relatively small.

In accordance with the basic premise of the p-α theory, Eq 31, the internal energy EOS for the granular material can be written as:

$$\varepsilon(v, \eta, \alpha) = \varepsilon_R + \varepsilon_s^{(\eta)}(v/\alpha; \eta_R) + C_{SR}^v \theta_R \chi_c(v/\alpha)[\omega_c(\eta) - 1] \tag{Eq 34}$$

Since the internal energy density EOS acts as a thermodynamic potential function, Eq 27 and 28, it can be used to derive the corresponding pressure and temperature EOSs for the granular material as:

$$p(v, \eta, \alpha) = \frac{1}{\alpha}\left[p_s^{(\eta)}(v/\alpha; \eta_R) + \sigma_R \chi_c(v/\alpha)[\omega_c(\eta) - 1]\right] \tag{Eq 35}$$

$$\theta(v, \eta, \alpha) = \frac{\partial \varepsilon(v, \eta, \alpha)}{\partial \eta} = \frac{\partial \varepsilon_s(v/\alpha, \eta)}{\partial \eta} = \theta(v/\alpha, \eta) = \theta_R \chi_c(v/\alpha)\omega_c(\eta) \tag{Eq 36}$$

where $\sigma_R = \rho_R \gamma_R C_{SR}^v \theta_R$.

Equation 34, 35, and 36 defines the sought energy, pressure, and temperature, EOSs, respectively, for the compacted granular material.

4.1.2 Pressure-Induced Yielding. The equations of state derived in the previous section describe the thermo-elastic response of the granular material, i.e., the response of this material in the absence of any inelastic effects. However, granular material compaction is an intrinsically irreversible process and requires additional considerations. As stated earlier, compaction is assumed to be controlled by pressure and it is further assumed to initiate at a critical pressure level commonly referred to as the pressure Hugoniot-elastic-limit ($p^{HEL} = p_{Y0}$). Also, it should be noted that when the pressure is removed (after compaction has initiated), only the thermoelastic portion of the deformation is recovered.

In this study, pressure-induced compaction of the granular materials is analyzed using the Boade model (Ref 9). Within the

Boade model, compaction is assumed to occur at a pressure p_{Y_0} when material porosity is α_{Y_0}. For a given parent material, p_{Y_0} and α_{Y_0} are specific to the initial (stress-free) material porosity $\alpha_R = v_R/v_{SR}$. Subsequent compaction requires an increased pressure $p_Y(\alpha)$ given by:

$$p_Y(\alpha) = p_{Y_0} - \hat{p}\ln\left(\frac{\alpha - 1}{\alpha_{Y_0} - 1}\right) \quad \text{(Eq 37)}$$

where $\hat{p}$ is another α_R-specific material parameter. Equation 37 simply states that as the pressure is increased above p_{Y_0}, granular material compacts (porosity decreases) to support the increased pressure.

Since the main objective of this study is to analyze the response of granular materials to shock loading, superscript HEL will be used in place of subscript Y_0 in the remainder of this article to denote the onset of pressure-induced densification.

4.1.3 Derivation of the Granular Material Hugoniot Relations. In this section, the granular material equations of state, Eq 34 to 36, are combined with the pressure-induced compaction equation, Eq 37, to derive the corresponding Hugoniot relations for this type of material. This is accomplished by applying the following procedure:

(a) First, Eq 34 and 31 are combined to eliminate the $\omega_c(\eta)$ term to get:

$$p(v,\eta,\alpha) = \frac{1}{\alpha}\left[p_s^{(\eta)}(v/\alpha;\eta_R) + \frac{\gamma_{SR}}{v_{SR}} \times \left[\varepsilon(v,\eta,\alpha) - \varepsilon_s^{(\eta)}(v/\alpha;\eta_R)\right]\right] \quad \text{(Eq 38)}$$

Note that if α is transferred to the left-hand side of Eq 38 then via Eq 34 and 35 becomes a simple statement of the p-v-ε Mie-Gruneisen EOS for the parent material with $v_s = v/\alpha$.

(b) Next, Eq 38 is used to define the associated granular material pressure versus specific volume Hugoniot. Note that one can think of the $p(v,\eta,\alpha)$ EOS defined by Eq 38 as a hyper-surface (within a p, η, α space) while the Hugoniot

$$p^{(H)}(v) = \frac{1}{\alpha}p_s^{(\eta)}(v/\alpha;\eta_R) + \frac{\gamma_{SR}}{\alpha v_{SR}}\left[\varepsilon^{(H)}(v) - \varepsilon_s^{(\eta)}(v/\alpha;\eta_R)\right] \quad \text{(Eq 39)}$$

is a hyper-line lying on this surface. The isentrope $(1/\alpha)\cdot p_s^{(\eta)}(v,\eta,\alpha)$ appearing in Eq 39 can also be treated as a hyper-line on the $p(v,\eta,\alpha)$ hyper-surface. The same can be said for the $\varepsilon_s^{(\eta)}(v,\eta,\alpha)$ isentrope which lies on the $\varepsilon(v,\eta,\alpha)$ hyper-surface.

Equation 39 contains on its right-hand side one Hugoniot relation, two isentropes and porosity, α, which must all be evaluated before the pressure Hugoniot for the granular material can be determined;

(c) Towards that end, $\varepsilon^{(H)}(v)$ is eliminated from Eq 39 through the use of the Rankine-Hugoniot equation as

$$\varepsilon^{(H)}(v,\alpha) = \varepsilon^{HEL} + \frac{1}{2}\left[p^{(H)}(v,\alpha) + p^{HEL}\right]\left(v^{HEL} - v\right) \quad \text{(Eq 40)}$$

where the Hugoniot is centered about the HEL state, the state at which compaction of the granular material begins.

Substitution of Eq 40 into 39 yields:

$$p^{(H)}(v) = \left\{\frac{1}{\alpha}p_s^{(\eta)}(v/\alpha;\eta_R) - \frac{\gamma_{SR}}{\alpha v_{SR}}\varepsilon_S^{(\eta)}(v/\alpha;\eta_R) + \frac{\gamma_{SR}}{\alpha v_{SR}}\left[\varepsilon^{HEL} + \frac{1}{2}p^{HEL}\left(v^{HEL} - v\right)\right]\right\} \times \left[1 - \frac{\gamma_{SR}}{2\alpha v_{SR}}\left(v^{HEL} - v\right)\right]^{-1}. \quad \text{(Eq 41)}$$

(d) The next step is to determine the two isentropes appearing in Eq 41. However, before this is done one must recognize that Eq 27 and 29 which relate pressure and internal energy density between the granular material and its parent matter impose some restrictions on the isentropes in question. To show this Eq 41 is evaluated at $v = v^{HEL}$, $\eta = \eta^{HEL}$, and $\alpha = \alpha^{HEL}$ to get

$$p^{HEL} = \frac{1}{\alpha^{HEL}}\left[p_s^{(\eta)}\left(v_s^{HEL};\eta_s^{HEL}\right) - \frac{\gamma_{SR}}{v_{SR}}\varepsilon_s^{(\eta)}\left(v_s^{HEL};\eta_s^{HEL}\right) + \frac{\gamma_{SR}}{v_{SR}}\varepsilon^{HEL}\right], \quad \text{(Eq 42)}$$

It should be noted that the two isentropes are now chosen in such a way that they pass through the HEL state. This is done to ensure that, in accordance with Eq 27 and 29, the following conditions hold:

$$\frac{1}{\alpha^{HEL}}p_s^{(\eta)}\left(v_s^{HEL};\eta_s^{HEL}\right) = p^{HEL} \quad \text{(Eq 43)}$$

$$\varepsilon_s^{(\eta)}\left(v_s^{HEL};\eta_s^{HEL}\right) = \varepsilon^{HEL} \quad \text{(Eq 44)}$$

(e) At this point, the pressure isentrope of the granular material can be evaluated by relating it to the (known) principal Hugoniot of the parent matter as

$$p_s^{(\eta)}\left(v_s;\eta_s^{HEL}\right) = \chi_c(v_s)\left[p_s^{HEL} + \int_{v_s^{HEL}}^{v_s}\frac{k_c(v')}{\chi_c(v')}\,dv'\right] \quad \text{(Eq 45)}$$

where,

$$\chi_c(v_s) = \exp\left[\frac{\gamma_{SR}}{v_{SR}}\left(v_s^{HEL} - v_s\right)\right] \quad \text{(Eq 46)}$$

$$k_c(v_s) = \frac{\gamma_{SR}}{2v_{SR}}p^{HS}(v_s) + \left[1 - \frac{\gamma_{SR}}{2v_{SR}}\left(v_s^{HEL} - v_s\right)\right]\frac{dp^{HS}(v_s)}{dv_s} \quad \text{(Eq 47)}$$

The known $p^{(HS)}(v)$ Hugoniot is assumed to be defined by the known Eulerian shock speed versus particle velocity relation defined earlier and the shock jump equations as:

$$p^{HS}(v_s) = \frac{(\rho_{SR}C_B)^2(v_{SR} - v_s)}{\left[1 - \rho_{SR}S(v_{SR} - v_s)\right]^2} \quad \text{(Eq 48)}$$

(f) Using the basic energy balance equation, the remaining energy density isentrope can be defined as:

$$\varepsilon_s^{(\eta)}\left(v_s, \eta_s^{HEL}\right) = \varepsilon_s^{HEL} - \int_{v_s^{HEL}}^{v_s} p_s^{(\eta)}\left(v', \eta_s^{HEL}\right) dv' \quad \text{(Eq 49)}$$

(g) The next task is to determine the porosity α as a function of v of the granular material since α also appears in the Hugoniot relations, Eq 41. It should be noted that the Hugoniot pressure at any level of v is balanced by the irreversible compaction granular material strength, Eq 37 and thereby equating the two one gets:

$$p^{HEL} - \hat{p}\ln\left(\frac{\alpha-1}{\alpha^{HEL}-1}\right) = \left\{\frac{1}{\alpha}p_s^{(\eta)}(v/\alpha;\eta_s^{HEL}) - \frac{\gamma_{SR}}{\alpha v_{SR}}\varepsilon_s^{(\eta)}(v/\alpha;\eta_s^{HEL}) + \frac{\gamma_{SR}}{\alpha v_{SR}} \times \left[\varepsilon^{HEL} + \frac{1}{2}p^{HEL}\left(v^{HEL}-v\right)\right]\right\}\left[1 - \frac{\gamma_{SR}}{2\alpha v_{SR}}\left(v^{HEL}-v\right)\right]^{-1} \quad \text{(Eq 50)}$$

Equation 50 has to be solved numerically to obtain the sought $\alpha(v)$ relationship. Then this relationship along with the two isentropes, Eq 45 and 49, respectively, can be used to obtain the sought $p^H(v)$ Hugoniot, Eq 41.

An example of the pressure versus specific volume Hugoniot results obtained in the case of porous copper (the relevant data given in Table 1) is displayed in Fig. 6(a). Once the pressure Hugoniot is derived, the corresponding energy-density Hugoniot can be obtained via Eq 40. Next, the temperature Hugoniot is obtained by evaluating Eq 36 along the Hugoniot line, while defining the $\omega_c(\eta)$ term using the pressure Hugoniot relation Eq 35 to get:

$$\theta^{(H)}(v) = \theta_R\chi_c(v/\alpha) + \frac{v_{SR}}{C_{SR}^v\gamma_{SR}}\left[\alpha p^{(H)}(v) - p_s^{(\eta)}\left(v/\alpha;\eta_s^{HEL}\right)\right] \quad \text{(Eq 51)}$$

Table 1 Properties of solid/parent material (Ref 15) and the granular material (Ref 1)

Parameter	Unit	Value
Solid/parent material (Ref 15)		
ρ_{SR}	kg/m^3	8930
C_B	m/s	3940
S	…	1.489
γ_{SR}	…	1.99
C_{SR}^v	J/(kg·k)	392.7
θ_R	K	293
ε_R	J/kg	77,732
Granular material (Ref 1)		
ρ_R	kg/m^3	6430
α_R	…	1.389
p^{HEL}	GPa	0.135
v^{HEL}	m^3/kg	1.546×10^{-4}
α^{HEL}	…	1.382
$\hat{p}$	GPa	0.394
ε^{HEL}	J/kg	77,792

Finally, the entropy-density Hugoniot is obtained by combining Eq 33, 35, and 51 to yield:

$$\eta^{(H)}(v) = \eta^{HEL} + C_{SR}^v \ln\left[\frac{\theta^{(H)}(v)}{\theta_R\chi_c(v/\alpha)}\right] \quad \text{(Eq 52)}$$

Equation 52 will be used in the next section since unloading takes place along an isentrope. An example of the temperature and entropy-density versus specific volume Hugoniot results obtained in the case of porous copper is displayed in Fig. 6(b) and (c), respectively.

4.2 Unloading Stage

It is generally accepted that when granular material is fully compacted (zero-porosity condition) during loading, unloading involves only the thermo-elastic decompression of the fully compacted material along an isentrope. In partially compacted granular material, on the other hand, one expects in addition to thermo-elastic decompression, some level of porosity recovery will accompany unloading (also taking place along an isentrope).

In the remainder of this section, a simple procedure is derived which can be used to assess the state of the partially compacted granular material upon unloading to a pressure $p^{++} = 0$. Since, the unloading isentrope is generally quite steep relative to the Hugoniot, it will be assumed (without a significant loss in fidelity) to be a straight line between the granular material "+" state (attained at the end of loading) to the "++" state attained after unloading.

The value of the entropy density along the decompression isentrope, $\eta^+ = \eta^{++}$, is defined by Eq 52. To completely define the "++" state of the compacted granular material the following procedure is employed:

(a) First, v_s^{++} is determined using Eq 35 in which $p(v = v^{++}, \eta = \eta^{++}, \alpha = \alpha^{++}) = 0$, as:

$$p_s^{(\eta)}\left(v_s^{++};\eta_R\right) + \sigma_R\chi_c\left(v_s^{++}\right)\left[\omega_c(\eta^{++}) - 1\right] = 0 \quad \text{(Eq 53)}$$

and Eq 53 is solved numerically for $v_s^{++}(= v^{++}/\alpha^{++})$.

(b) Next, v_s^{++} is used in Eq 34 to get ε^{++}.

(c) Finally to get v^{++}, it is assumed that the pressure isentrope in question can be approximated with a shock centered about the "++" state. Using the Lagrangian form of the linear-momentum and energy shock jump conditions:

$$(\rho_{SR}U_s)^2(v^{++} - v^+) = p^+ \quad \text{(Eq 54)}$$

$$\frac{1}{2}p^+(v^{++} - v^+) = \varepsilon^+ - \varepsilon^{++} \quad \text{(Eq 55)}$$

one can get v^{++} and u_s as:

$$v^{++} = v^+ + \frac{2(\varepsilon^+ - \varepsilon^{++})}{p^+} \quad \text{(Eq 56)}$$

and

$$u_s = U_s + \dot{x}^+ = \left(\frac{(p^+)^2}{2\rho_{SR}^2(\varepsilon^+ - \varepsilon^{++})}\right)^{\frac{1}{2}} + \dot{x}^+. \quad \text{(Eq 57)}$$

Once the v^{++} is determined, relations analogous to those appearing in Eq 18 and 24 can be used to define ε^{++} and θ^{++}.

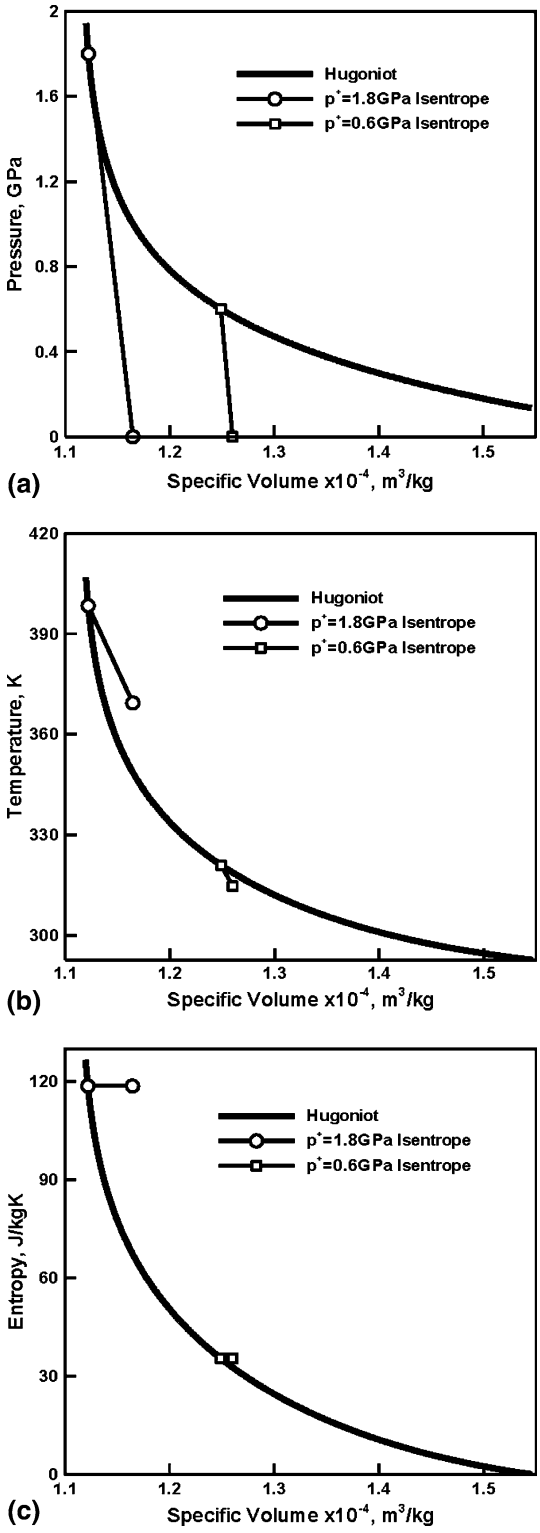

Fig. 6 (a) Pressure; (b) temperature; and (c) entropy Hugoniots and isentropes for granular copper with an initial degree of distention of $v_R/v_{SR} = 1.5$, loaded with a flat-topped pressure pulse in the moderate shock regime

An example of the pressure versus specific volume isentropes obtained in the case of porous copper (the relevant data given in Table 1) is displayed in Fig. 6(a). The corresponding temperature and entropy density versus specific volume isentropes are displayed in Fig. 6(b) and (c), respectively.

4.3 Moderate Shock-Attenuation/Energy-Dissipation Potential of Granular Materials

As in the case of the strong shock, the shock attenuation potential of a granular material is controlled by the relative magnitudes of the shock speed and the average decompression wave speed. The same combination of material properties as listed in section 3.3 is desirable in the case of moderate shock attenuation and the associated energy-dissipation. However, in the moderate shock regime, additional material parameters (those related to the compaction process) affect the granular material's shock attenuation and energy-dissipation potential.

A parametric study involving the three Boade compaction model (Ref 9) parameters: p_{Y_0}, $\hat{p}$ and α_{Y_0}, carried as part of the present work identified $\hat{p}$ as having the most significant effect on the shock-attenuation/energy-dissipation potential of granular materials in the moderate shock regime. This finding is reasonable considering the fact that p_{Y_0} generally remains small relative to the shock strength even if its magnitude is increased using a single digit multiplier. Also, since α_{Y_0} is the argument of a natural logarithm function, its effect is diminished. As far as $\hat{p}$ is concerned, smaller values (which yield Hugoniots with lower slopes and thus result in lower shock speeds) are preferred. Thus, a low value of $\hat{p}$ should be added to the list of desirable material attributes described in section 3.3 for materials to be used in shock-mitigation and energy-dissipation applications.

5. Discussion

The analysis presented in the last three sections established identification of the important properties of granular materials (and their parent matter) which control the ability of the materials to efficiently attenuate planar shocks and dissipate the energy carried by them, in each of the three shock-loading regimes considered. It could be argued that many of these properties could have been identified using simple physical arguments and the knowledge of the basic phenomena accompanying flat-topped pulse shock loading. For example, no detailed shock-physics-based analysis was needed to identify a high level of granular materials distension as a desired property of this material from the standpoint of efficient shock attenuation/energy-dissipation.

However, the detailed analysis of flat-topped pulse shock loading enables a direct comparison of shock-attenuation/energy-dissipation efficiencies of two of more candidate materials. This analysis can next be combined with an optimization-based material selection procedure (Ref 10-14). In this case, the objective of material selection procedure could be minimization of the weight of a granular-material protective structure which can fully attenuate (or reduce the intensity below a safe threshold) a shock resulting from a flat-topped pulse loading. This procedure is currently under development and will be reported in our future communication.

6. Summary and Conclusions

Based on the results obtained in this study, the following main summary remarks and conclusions can be drawn:

1. Three regimes of shock loading of granular materials are identified and analyzed.

2. In the first, low-strength/weak-shock regime, the effect of material strength can be neglected and the granular material in then assumed to be fully compacted at any shock-strength level within this regime. The efficiency of shock-attenuation/energy-dissipation of a granular material in this regime is found to be solely controlled by the extent of material distension.
3. In the strong shock regime, shock strength is so high that the granular material is fully compacted and, in addition, thermo-elastically compressed. In this shock-loading regime, additional material parameters (e.g., particle-velocity dependence of the shock speed, Gruneisen gamma parameter, etc.) affect granular materials' shock-attenuation/energy-dissipation potential.
4. In the moderate-shock regime, details of the compaction process within the granular material need to be considered. Consequently, parameters related to the compaction process also affect granular materials' shock-attenuation/energy-dissipation potential.

Acknowledgments

The material presented in this article is based on work supported by the Office of Naval Research (ONR) research contract entitled "*Elastomeric Polymer-By-Design to Protect the Warfighter Against Traumatic Brain Injury by Diverting the Blast Induced Shock Waves from the Head*", Contract Number 4036-CU-ONR-1125 as funded through the Pennsylvania State University. The authors are indebted to Dr. Roshdy Barsoum of ONR for continuing support and interest in the present work. The authors would also like to thank Dr. Lee Davison whose book "*Fundamentals of Shock Wave Propagation in Solids*" and specifically Chapter 11: Porous Solids, provided the motivation and the necessary shock-physics background used in the present work.

Appendix: Strong-Shock Temperature Hugoniot

The procedure described in this appendix enables calculation of the temperature Hugoniot from the known stress/pressure Hugoniot for the granular material in the strong shock regime, as well as for its parent material. First, the Rankine Hugoniot equation is defined as:

$$\varepsilon^{(\mathrm{H})}(v) = \varepsilon^{-} + \frac{1}{2}\left[p^{(\mathrm{H})}(v) + p^{-}\right](v^{-} - v) \qquad \text{(Eq A.1)}$$

and differentiated to get:

$$\frac{\mathrm{d}\varepsilon^{(H)}(v)}{\mathrm{d}v} = \frac{1}{2}\left[(v^{-} - v)\frac{\mathrm{d}p^{(\mathrm{H})}(v)}{\mathrm{d}v} - p^{(\mathrm{H})}(v) - p^{-}\right] \qquad \text{(Eq A.2)}$$

Then, the following expression for the combined First and Second Law of Thermodynamics along the Hugoniot:

$$\frac{\mathrm{d}\varepsilon^{(H)}(v)}{\mathrm{d}v} = \theta^{(\mathrm{H})}(v)\frac{\mathrm{d}\eta^{(\mathrm{H})}(v)}{\mathrm{d}v} - p^{(\mathrm{H})}(v) \qquad \text{(Eq A.3)}$$

is combined with Eq A.2 to eliminate $\frac{\mathrm{d}\varepsilon^{(H)}(v)}{\mathrm{d}v}$ and get:

$$\frac{\mathrm{d}\eta^{(\mathrm{H})}(v)}{\mathrm{d}v} = \frac{\kappa(v)}{2\theta^{(\mathrm{H})}(v)} \qquad \text{(Eq A.4)}$$

where $\kappa(v) = p^{(\mathrm{H})}(v) - p^{-} + (v^{-} - v)\frac{\mathrm{d}p^{(\mathrm{H})}(v)}{\mathrm{d}v}$.

To obtain the temperature Hugoniot, $\eta^{(\mathrm{H})}(v)$ must be eliminated from Eq A.4. Toward that end, the total derivative of the temperature is defined using the known thermodynamic derivatives (Ref 1) as:

$$\mathrm{d}\theta = \left.\frac{\partial\theta}{\partial v}\right|_{\eta}\mathrm{d}v + \left.\frac{\partial\theta}{\partial\eta}\right|_{v}\mathrm{d}\eta = -\theta\frac{\gamma(v)}{v}\mathrm{d}v + \frac{\theta}{c^{v}(\eta)}\mathrm{d}\eta \qquad \text{(Eq A.5)}$$

or

$$\frac{\mathrm{d}\theta^{(H)}(v)}{\mathrm{d}v} = -\frac{\gamma(v)}{v}\theta^{(\mathrm{H})}(v) + \frac{1}{C^{v}(\eta^{(\mathrm{H})}(v))}\theta^{(\mathrm{H})}(v)\frac{\mathrm{d}\eta^{(H)}(v)}{\mathrm{d}v} \qquad \text{(Eq A.6)}$$

using Eq A.4, (Eq A.6) becomes

$$\frac{\mathrm{d}\theta^{(\mathrm{H})}(v)}{\mathrm{d}v} + \frac{\gamma(v)}{v}\theta^{(\mathrm{H})}(v) = \frac{\kappa(v)}{2C_{\mathrm{R}}^{v}} \qquad \text{(Eq A.7)}$$

Equation A.7 is a first-order ordinary differential equation (ODE) in the quadrature format (since its second term is a product of a function of the independent variable v and the dependent variable, $\theta^{(\mathrm{H})}(v)$. These types of ODE's are integral in a disguised format and can be readily integrated. The integrated form of Eq A.7 is given in Eq 15.

References

1. L. Davison, *Fundamentals of Shock Wave Propagation in Solids*, Springer, Berlin, Heidelberg, Germany, 2008
2. S.P. Medvedev, S.M. Frolov, and B.E. Gel'fand, Attenuation of Shock-Waves by Screens of Granular Materials, *J. Eng. Phys. Thermophys.*, 1990, **58**(6), p 714–718
3. J. Bakken, T. Slungaard, T. Engebretsen, and S.O. Christensen, Attenuation of Shock Waves by Granular Filters, *Shock Waves*, 2003, **13**(1), p 33–40
4. A.B. Sawaoka, Dynamic Consolidation of Non-Oxide Ceramic Powders, *Physica B*, 1986, **139–140**(3), p 809–812
5. A.H. Shen, T.J. Arhens, and J.D. O'Keefe, Shock Wave-Induced Vaporization of Porous Solids, *J. Appl. Phys.*, 2003, **93**(9), p 5167–5174
6. M.V. Muniz, H. Sobral, and R.N. Gonzalez, Shock and Thermal Wave Study of Laser-induced Plasmas in Air by the Probe Beam Deflection Techniques, *Meas. Sci. Technol.*, 2003, **14**, p 614–618
7. J.R. Rempel, D.N. Schmidt, J.O. Erkman, and W.M. Isbell, *Shock Attenuation in Solids and Distended Materials*, Stanford Research Institute, Report No. AD0628796, 1965
8. R.F. Trunin, K.K. Krupnikov, G.V. Simakov, and A.I. Funtikov, Shock-Wave Compression of Porous Metals, *High-Pressure Shock Compression of Solids VII—Shock Waves and Extreme States of Matter*, Springer, New York, p 177–195, 2004
9. R.R. Boade, Principal Hugoniot, Second-Shock Hugoniot, and Release Behavior of Pressed Copper Powder, *J. Appl. Phys.*, 1970, **41**(11), p 4542–4551
10. M.F. Ashby, *Material Selection in Mechanical Design*, 3rd ed., Butterworth-Heinemann, 2005
11. M. Grujicic, V. Sellappan, T. He, N. Seyr, A. Obieglo, M. Erdmann, and J. Holzleitner, Total Life-Cycle Based Materials Selection for Polymer Metal Hybrid Body-In-White Automotive Components, *J. Mater. Eng. Perform.*, 2009, **18**, p 111–128
12. M. Grujicic, G. Arakere, V. Sellappan, A. Vallejo, and M. Ozen, Structural-response Analysis, Fatigue-life Prediction and Material Selection for 1 MW Horizontal-axis Wind-Turbine Blades, *J. Mater. Eng. Perform.*, 2010, **19**(6), p 780–801
13. M. Grujicic, G. Arakere, X. Xie, M. LaBerge, A. Grujicic, D.W. Wagner, and A. Vallejo, Design optimization and Material Selection for a Femoral-Fracture Fixation-Plate Implant, *Mater. Des.*, 2010, **31**, p 3463–3473

14. M. Grujicic, X. Xie, G. Arakere, A. Grujicic, D.W. Wagner, and A. Vallejo, Design-Optimization and Material Selection for a Proximal Radius Fracture-fixation Implant, *J. Mater. Eng. Perform.*, 2010, **19**(8), p 1090–1103

15. R.G. McQueen, S.P. Marsh, J.W. Taylor, J.N. Fritz, and W.J. Carter, The Equation of State of Solids from Shock Wave Studies, *High Velocity Impact Phenomena*, R. Kinslow, Ed., New York, Academic Press, 1970, p 293–417